Heliyon 8 (2022) e09103

Contents lists available at ScienceDirect

Heliyon

journal homepage: www.cell.com/heliyon

Research article

Synergistic combination of PMBA and 5-fluorouracil (5-FU) in targeting mutant KRAS in 2D and 3D colorectal cancer cells

Arem Qayum [a,b,*], Asmita Magotra [c], Syed Mohmad Shah [e], Utpal Nandi [c], P.R. Sharma [a], Bhahwal Ali Shah [d], Shashank Kumar Singh [a,**]

[a] Cancer Pharmacology Division, Indian Institute of Integrative Medicine, CSIR, Jammu, 180001, India
[b] Academy of Scientific and Innovative Research (AcSIR), Ghaziabad, 201002, India
[c] PK-PD, Toxicology and Formulation Division, Indian Institute of Integrative Medicine, CSIR, Jammu, 180001, India
[d] Natural Product Microbes Division, Indian Institute of Integrative Medicine, CSIR, Jammu, 180001, India
[e] Sher-e-Kashmir University of Agricultural Sciences & Technology of Kashmir, Srinagar, 190001, India

GRAPHICAL ABSTRACT

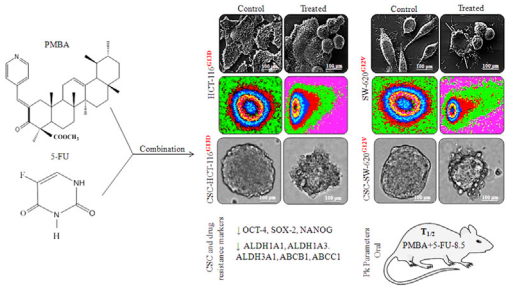

ARTICLE INFO

Keywords:
Colon cancer
PMBA
5-fluorouracil
KRAS
Spheroid-formation (colonospheres)
Combination study
Pharmacokinetics

ABSTRACT

β-Boswellic acid (β-BA), a potent NF-kB signaling pathway inhibitor, has shown synergistic anti-cancerous activity (NCT03149081, NCT00243022 and NCT02977936) in various clinical trials as complementary therapies. The study has been conducted to investigate the effect and efficacy of 2-pyridin-4-yl methylene β-boswellic acid (PMBA) and 5-Flourouracil (5-FU) in combination therapy for the treatment of KRAS mutant colon cancer. Analysis of isobologram showed synergistic combination index (CI $>$ 1) of PMBA and 5-FU against the HCT-116^{G13D} and SW-620^{G12V} cell lines. The growth-inhibiting PMBA also caused apoptosis mediating effects with dose-dependent increase in caspase-3 activity, while inhibiting the formation of colonies in combination with 5-FU. As evident, PMBA affected colorectal 3D CSC properties including the ability to self-renew along with the expression of multi-drug resistance genes, *viz.*, ABCB1, ABCC1 and ALDH1A1, ALDH1A2, ALDH1A3, ALDH3A1, and CSC markers like CD44, CD166, EPCAM, OCT-4, SOX-2, and NANOG compared with those in 2D model explaining the expression pattern of oncogenic KRAS$^{G13D,\ G12V}$ mutation. When examined for plasma level of PMBA (20 mg) and PMBA+5-FU (20 + 40 mg), a time-dependent increase in the level of the drug (5-FU) was detected, indicating its absorption and bioavailability with excellent half-life of the PMBA for both routes of administration (IV and Oral), thereby indicating a new adjuvant therapy for KRAS mutant colon cancer.

* Corresponding author.
** Corresponding author.
E-mail addresses: aremqayoom03@gmail.com (A. Qayum), sks@iiim.ac.in (S.K. Singh).

https://doi.org/10.1016/j.heliyon.2022.e09103
Received 7 October 2021; Received in revised form 12 November 2021; Accepted 9 March 2022

1. Introduction

Among all cancer types, colon cancer is the second leading cause of death worldwide accounting to 19.3 million cases and 10 million deaths by 2020 (GLOBOCAN). Various limitations in the on-going therapies are due to resistance imposed by cancer cells to chemotherapeutic drugs, ultimately leading to reoccurrence with less improvement in the overall survival of the patients. The major chemo-therapeutic approaches of mono and combination regimens used to treat cancer have not been consistently successful due to non-selectivity and early attainment of drug resistance and recruitment of other salvage pathways by the cancer cells (Mokhtari et al., 2017). The combination therapy, however, holds a greater potential for controlling cancer, primarily due to its steady evolution in usage and application of new substances, especially of natural origin. The progressive increase in the applicable knowledge of cancer biology, pharmacology and toxicology improved the design of clinical trials and their combinatorial use with early stages of the disease (Doroshow and Simon, 2017). Also, several natural compounds have been investigated for their ability to improve the chemo-sensitizing effects of 5-FU in colorectal cancer (Afrin et al., 2018, 2021).

In combination therapy, the interaction of drug becomes more effective when the sum of combined drug exhibits synergism in which the effect is greater than the sum of the effects of the single agents used, thereby producing $1 + 1 > 2$ effect. In the scheme of isobologram analysis, various parameters include: Additive ($CI = 1$)- when the combined effect of drug A and drug B is equal to the individual effect exhibited by drug A and drug B; Synergism ($CI < 1$)-when the combined effect of drug A and drug B is more than the individual effect exhibited by drug A and drug B; and Antagonism ($CI > 1$) when the combined effect of drug A and drug B is less than the individual effect of drug A and drug B (Ting-Chao Chou, 2010). The use of combination drugs in animal and/or clinical application provides the required thrust, as the therapeutic effect of combined drugs is generally proven better than that of a monotherapy. By combining agents, the synergistic promoting properties with favourable pharmacokinetic (PK) makes it possible to decrease the dose and/or dosing frequency of the drug in order to achieve blood concentrations of the combination sufficient for cancer growth suppression. The initial combination-screening is easily possible in *in-vitro* analysis which can help to predict which drug interactions will occur at the therapeutic doses in order to identify drug combinations with favourable PK profiles worthy of evaluation in clinical trials. Constitutive activation of RAS/RAF/MEF/ERK pathway in cancerous cells renders EGFR inhibitors, first generation TKIs Geftinib and Erlotinib, ineffective with loss of control over EGFR signaling (Eberhard et al., 2005). Likewise, in EGFR monotherapy, due to downstream KRAS mutation, none of the TKI drug (tyrosine kinase inhibitors) is effective, accounting for no EGFR drug is in compilation till date (Roberts and Der, 2007). However, combination therapy came into existence due to less toxicity imposed on normal cells with multiple targets. Also, achieve a low therapeutic dosage of drug which is synergistic in nature and increased therapeutic index providing more potent effect. Various combination regimens used for colon cancer treatment like, CAPOX (Osawa et al., 2014), FOLFIRI (Lu et al., 2014), FOLFIRI-CETUXIMAB (Heinemann et al., 2021), FOLFOX (Schultheis et al., 2013), FOLFIRI-BEVACIZUMAB (Beretta et al., 2013), FU-LV (Gramont et al., 2000), XELIRI (Delord et al., 2005), and XELOX (Cassidy et al., 2004), etc. have been found to be effective and successful.

5-Fluorouracil (5-FU) though having worked as an anti-metabolite chemotherapeutic agent for the colorectal cancer treatment has taken a backseat due to several limitations pertaining to its low bioavailability and short half-life (Zhang et al., 2008). To overcome the drawbacks of 5-FU, comprehensive research has been conducted to enhance its therapeutic efficiency in order to successfully deliver 5-FU to tumor sites (Almahdi et al., 2020). The inability of single agent chemotherapy to eliminate CSCs has again diverted the focus towards combination-drug targeting of CSCs. A combination of Salinomycin and Docetaxel, and Thymoquinone (TQ) and 5-FU has been shown to effectively kill gastric CSCs by preventing drug resistance and reoccurrence (Yang et al., 2020). The main cause of relapse is the subpopulation of cancer stem cells (CSCs) which give rise to chemo-resistance to a large extent bestowing tumor the invasive and differentiation potential. A target based broad cell line (NCI-60) profiling from diverse panel of cancer tissues revealed synergistic efficacy of PMBA in $KRAS^{G13D,\ G12V}$ mutant colon cancer cell lines. In the present study, observation has been extended to combination therapy to treat colon cancer, particularly KRAS mutated colon cancer. Among the 21 in-house novel β-boswellic acid derivatives, PMBA was found to be the most potent cytotoxic candidate with selectivity in killing KRAS mutant colon cancer cells (Kumar et al., 2016). In the current scenario, various combinations of PMBA and 5-FU have been analyzed for their potential to target KRAS mutant colon cancer cell with the hypothesis that the combinatorial therapy would provide a more efficient regimen for treatment of the cancer.

2. Materials and methods

2.1. SRB assay

In 96-well micro-titer plates, cells- HCT-116^{G13D} and SW-620^{G12V} (obtained from the NCI-Frederick cancer-DCTD cell line repository) were seeded at densities ranging from 5000 to 10,000 cells/100 μL/well, depending on the doubling time. Then, PMBA was added after the completion of 24 h (using a 7-point dose scale diluted 2-fold) and further incubated for various time points (24, 48 and 72 h) at different concentrations. Paclitaxel was used as a positive control. Then, plates were incubated under the same conditions for 48 h at 37 °C. After incubation, the cells were fixed with TCA for 1 h at 4 °C. The plates were then washed, thrice, with water and allowed to air dry. Using 100 μL of 0.4% SRB dye, the plates were rinsed three times with water, followed by 1% v/v acetic acid to remove the unbound SRB. Following drying at room temperature, the dye was solubilized by adding 100 μL of 10 mM Tris buffer (pH 10.4). After 5 min, the plates were shaken so that the protein-bound dye would dissolve. OD readings were taken at 540 nm using a microplate reader (Thermo Scientific) and IC_{50} was determined using the software GraphPAD Prism Version 5.0. The assay was performed in quadruplicates (Kumar et al., 2016).

2.2. Colony formation assay

HCT-116^{G13D} and SW-620^{G12V} cells (7.5×10^4/mL/well) were seeded and treated with PMBA (1.7, 2.2 μM), 5-FU (14.7, 78 μM) and PMBA+5-FU ($1.7 + 14.7$, $2.2 + 78$ μM) at different concentrations for 24 h. The treated cells were trypsinized, counted and re-seeded at 1000 cells/well in a six-well plate, so as to have colonies of >50 cells to analyse the colonogenic ability of both the cell lines. Subsequently, cells were fixed with 1 mL of 4% formaldehyde and stained with 0.5% crystal violet. Eventually, crystal violet stain was aspirated carefully followed by thorough rinsing with water three to five times. Then, colonies were expressed as the number of colony-forming units in treated cells in comparison to untreated controls (Crowley et al., 2016).

2.3. Scanning electron microscopy

HCT-116^{G13D} and SW-620^{G12V} monolayers incubated with PMBA (1.7, 2.2 μM), 5-FU (14.7, 78 μM) and PMBA+5-FU ($1.7 + 14.7$, $2.2 + 78$ μM) for 48 h on serum-coated coverslips were treated for 30 min, fixed at 37 °C (4% formaldehyde, 2.5% glutaraldehyde, 0.1 M sodium cacodylate, pH 7.4) and washed 3X with PBS and post-fixed with buffered 1% Osmium tetraoxide (OsO_4) for 3 h. Samples were then dehydrated through a graded ethanol series (30, 50, 70, 80, 90, 95, $2 \times 100\%$) followed by hexamethyldisilazane (HMDS), and critically point dried. The dried samples were coated with platinum-palladium alloy using sputter coater (JEOL JEC-300

FC, Japan). Images were acquired under scanning electron microscopy (JEOL JSMIT-300, Tokyo, Japan) (Fischer et al., 2012).

2.4. Caspase 3/7 activation assay

HCT-116^{G13D} and SW-620^{G12V} adherent cells following treatment were rinsed with ice-cold PBS, cell lysis buffer was added and left on ice for 5 min. Cells were scraped off and transferred to an appropriate tube. Lysates were sonicated and microcentrifuge for 10 min at 4 °C. Subsequently, the supernatant was transferred to the respective tubes. Caspase-3/7 activity was determined using the caspase-3 fluorescent assay kit (CST #5723) according to manufacturer's instructions, in 100 μg/well of total lysate protein of HCT-116^{G13D} and SW-620^{G12V} after treatment with PMBA (1.7, 2.2 μM), 5-FU (14.7, 78 μM) and PMBA+5-FU (1.7 + 14.7, 2.2 + 78 μM).

2.5. Comet assay

Cells were treated with PMBA, 5-FU or both for 48 h. The DNA damage was analyzed by SCGE as described (Lu et al., 2017; Shaker and Melake 2012). Cells were embedded in 75 μL of 0.5% low-melting-point agarose and microscope slides were immersed in ice-cold lysis buffer (2.5M NaCl, 100 mM EDTA, 10 nM Tris, 1% sodium laurylsarcosine (pH 10), 1% Triton X-100 and 10% DMSO) for 80 min. The slides were exposed to alkali (300 mM NaOH and 1 mM EDTA (pH > 13)) for 40 min. After electrophoresis (25 V, 300 mA, 15 min), the slides were neutralized in 0.4 M Tris buffer (pH 7.5). The ethidium bromide-stained slides were analyzed using an image analysis system. Comet tails were measured using the Kinetic imaging Komet 5.5 assay software and quantified.

2.6. Drug combination assay

For combination synergy studies, cells were plated in 96-well plates (NUNC) and treated with varying concentration of the compound, either alone or in combination with the 2-fold co-dilution of both agents which were screened and compared to the single agent response curve for 48 h. Cell inhibition was determined using SRB dye (Sigma, 230162). Synergistic effects were determined for PMBA and 5-FU using the Bliss independence analysis method through Synergy finder and Calcusyn Version 2.0 (Ianevski et al., 2017; Bijnsdorp et al., 2011).

2.7. Colonosphere formation assay

HCT-116-CSC and SW-620-CSC were maintained as non-adherent colonospheres, grown either in ultra-low adhesion (ULA) plates (Grenier) or in standard uncoated 10 cm petri dishes. Stem cell media (SCM) composed of DMEM/F12 (500 mL), supplemented with fibroblast growth factor (FGF) (10 ng/mL), epidermal growth factor (EGF) (20 ng/mL), and 10 mL B27 supplement (Life Technologies). Cells were plated as single cell suspensions at low cell densities and re-supplemented with SCM every three to four days. Colonospheres were allowed to form for ten days before they were collected in 15 mL tubes and subsequently passaged. For passage, colonospheres were rinsed with PBS and mechanically dissociated by passaging through a 20G syringe to achieve a single cell suspension. Cells were centrifuged at 400xg for 4 min and re-suspended in SCM to achieve the appropriate cell density (Bahmad et al., 2018; Chu et al., 2009).

2.8. Western blotting

Colonospheres of both HCT-116^{G13D} and SW-620^{G12V} cells were treated with PMBA, 5-FU or both at 1.7/2.2, 14.7/78 μM for 48 h in presence and absence of EGF (10 ng/mL). The treated cells were lysed in RIPA lysis buffer (Sigma, R0278), supplemented with protease inhibitor mixture (Promega, G6521) and phosphatase inhibitor mix (Thermo, 78420). Lysates were centrifuged at 15,000 rpm for 15 min and protein concentration was determined by Coomassie protein assay (Thermo Scientific, 1856209). Equal amounts of 70 μg of protein were subjected to SDS-PAGE analysis and transferred to PVDF membrane (Millipore, IPVH00010). After blocking with 5% non-fat milk-TBS or 3% BSA-TBS (for phosphorylated antibodies) in blocking buffer, membranes were incubated overnight at 4 °C with the specific primary antibodies [p-c-Kit (CST #3391), c-Kit (CST #3074)], and subsequently incubated with secondary antibodies [anti-mouse IgG (CST #7076), and anti-Rabbit IgG (CST #7074)]. After incubation, the membranes were treated with chemiluminescent HRP substrate and exposed to X-ray film, as per the already established protocol (Kumar et al., 2016).

2.9. RNA extraction and real-time reverse transcriptase-polymerase chain reaction (RT-PCR)

Human colon cancer cell lines HCT-116^{G13D} and SW-620^{G12V} were seeded overnight and treated with PMBA and 5-FU either singly (9.45/10.7/25 μM) or in combination (1.7 + 14.7/2.2 + 78 μM each) for 48 h. Control cells were treated with DMSO (0.2% final concentration). Total RNA was extracted from confluent monolayers of parental cell lines and ten-day-old CSC colonospheres, as per manufacturer's protocol by using Tri-reagent (Sigma) and incubated with RNase free DNase. cDNA was synthesized, from an equal amount of RNA (3 μg), using RevertAid cDNA synthesis kit according to the manufacturer's instruction. SYBR green PCR amplification was performed using the StratageneMX3000p Real-time PCR System with specific set of primers as listed in Table using GAPDH as housekeeping gene. The concentration of RNA and purity was determined using the NanodropND-1000 (Thermo Scientific, USA) by measuring the absorbance at 230, 260 and 280 nm. RNA was diluted to a concentration of 250 ng/μL, aliquoted and stored at -80 °C. 1 μg of RNA was converted to cDNA using the iScriptcDNA Synthesis Kit (BioRad) according to the manufacturer's protocol. Samples were diluted in 60 μL of RNase free deionized water and stored at -20 °C. RNA was also extracted from confluent CSC cell lines grown in monolayer in either standard media or SCM. RT-PCR was performed as: initial denaturation for 2 min at 95 °C, followed by 40 cycles of 5 s at 95 °C; 5 s at 60 °C and for final extension 72 °C for 5 min (Nolan et al., 2006).

2.10. Pharmacokinetic study of PMBA through oral and IV route

Pharmacokinetic study of PMBA was carried out using healthy adult male Balb/c mice (20–22 gm) through single dose oral and intravenous (IV) route. Animals were kept in standard laboratory conditions with *ad-libitum* water for a period of one week, and fasted overnight before oral pharmacokinetic study. On the day of experimentation, animals were divided into two groups (25/group) for oral as well as IV administration, which were further subdivided into five subgroups containing five animals each for sparse sampling. Two blood samples were collected from each subgroup. Dose was prepared in 0.5% DMSO, 10% solutol HS-15 and 85% water (v/v) as solution form, and administered through oral route by oral gavage at 20 mg/kg or IV route by tail vein injection at 5 mg/kg, dose volume being was 10 mL/kg. Blood samples were collected from retro-orbital plexus at 0.083 (for IV only), 0.25 h, 0.5 h, 1 h, 2 h, 4 h, 6 h, 8 h, 10 h, 12 h (for oral only) and 24 h, in microcentrifuge tubes containing 5% (w/v) disodium EDTA. Each blood sample was centrifuged at 8000 rpm for 10 min, and 50 μl plasma from each tube was further processed with methanol (200 μL) for plasma protein precipitation. The sample was mixed thoroughly by vortexing for 2 min followed by centrifugation at 14000 rpm for 10 min at 4 °C. Organic layer was separated and transferred to inner vial for quantitation of PMBA by LC-MS/MS (Make: Shimadzu; Model: 8030, Japan). Sample concentration was determined based on the calibration curve prepared by spiking appropriate concentration of PMBA in blank plasma. Separation was achieved in Chromolith High Resolution RP-18e column (100 × 4.6 mm) using isocratic mobile phase composition of water containing 0.1% (v/v) formic acid and acetonitrile (50:50, v/v) at the flow rate of 0.5 mL/min.

Tandem mass spectrophotometer with electrospray ionization (ESI) source was operated in positive mode and quantitation of PMBA was performed on multiple reactions monitoring (MRM) mode with parent ion/product ion transition pairs of 558.4 > 118.9. Plasma concentrations of PMBA at respective time points were obtained and calculation was done for various pharmacokinetic parameters (C_{max}, maximum plasma concentration; T_{max}, time to reach maximum plasma concentration; $T_{1/2}$, elimination half-life; AUC0-t, area under the curve for plasma concentration from zero to the last measurable plasma sample time; AUC0-∞, area under the curve for plasma concentration from zero to time infinity; V_d, volume of distribution; Cl, clearance) by non-compartmental analysis using PK solution software (Summit Research Services, Colorado, USA) (Yempalla et al., 2015; Magotra et al., 2018).

2.11. Pharmacokinetic study for combination of PMBA and 5-FU in Balb/c mice through oral route

Single dose oral pharmacokinetic study of PMBA was carried out using healthy adult Balb/c mice (20–22 gm) after necessary approval from Institutional Animal Ethics Committee (IEAC no. 68/91/8/16) of CSIR-Indian Institute of Integrative Medicine, Jammu, India. Twenty animals were kept in standard laboratory conditions with water *ad libitum* for a period of one week before experimentation. Animals were fasted overnight and divided into four groups containing five animals per group on the day of experimentation. PMBA and 5-FU dose was prepared in 0.5% v/v DMSO, 10% v/v Solutol and Water (q.s) and administered through oral route at 20 mg/kg with dose volume of 10 mL/kg. Blood samples were collected from retro-orbital plexus at 0 (pre-dose), 0.25 h, 0.5 h, 1 h, 2 h, 4 h, 6 h, 8 h and 10 h in microcentrifuge tubes containing 5% (w/v) disodium EDTA. Blood samples were collected two times from each group to execute pharmacokinetic study using sparse sampling technique. Each blood sample was centrifuged at 8000 rpm for 10 min to obtain each of 50 μL plasma which was further processed with methanol (200 μL) for plasma protein precipitation. Then, sample was mixed thoroughly by vortexing for 2 min followed by centrifugation at 14000 rpm for 10 min at 4 °C. Organic layer was separated and transferred to HPLC vial for analysis. PMBA was dissolved in DMSO and diluted further with Methanol to obtain calibration curve (0.39–2000 ng/mL) by spiking appropriate amount into the blank plasma. Quantitation of PMBA was carried out using LC-MS/MS (Make:Shimadzu; Model:8030). Plasma concentrations of PMBA at respective time points were obtained and calculation was done for various pharmacokinetic parameters by non-compartmental analysis using PK solution software (Summit Research Services, Colorado, USA) (Dheer et al., 2019).

2.12. Quantification and statistical analysis

The results were expressed as mean ± standard error of mean (SEM). Significance between controls and treated samples was calculated using Student's t-tests. Significance between controls in different cell lines was calculated using one and two-way ANOVAs and t-tests. Statistical calculations were performed using GraphPad prism version 5.0 (Chicago, USA). All analyses used $p < 0.05$, $P < 0.01$, $P < 0.001$ for determining significance *, ** and *** respectively.

3. Results

3.1. PMBA inhibited proliferation of KRAS mutated colon cancer cell lines

On the basis of information obtained from the Sanger Institute COSMIC database, SRB assay has been performed on KRAS mutant colon cancer lines - HCT-116^{G13D} and SW-620^{G12V} (NCI-DCTD, USA. After 48 h treatment, PMBA exhibited potent inhibitory activity resulted in IC_{50} values of 1.7, 2.2 μM whereas 5-FU exhibited IC_{50} of 14.76 and 78.33 μM in HCT-116^{G13D} and SW-620^{G12V}.

3.2. PMBA restricted KRAS-mutant colorectal cancer growth

On apoptosis regulation, PMBA remarkably induced cell apoptosis disrupting cellular integrity in KRAS mutant colon cancer cell lines-HCT-116^{G13D} and SW-620^{G12V} by inducing ~20 times increased expression of caspase-3 activity (Figure 1B,C), indicating that caspase-3 expression is

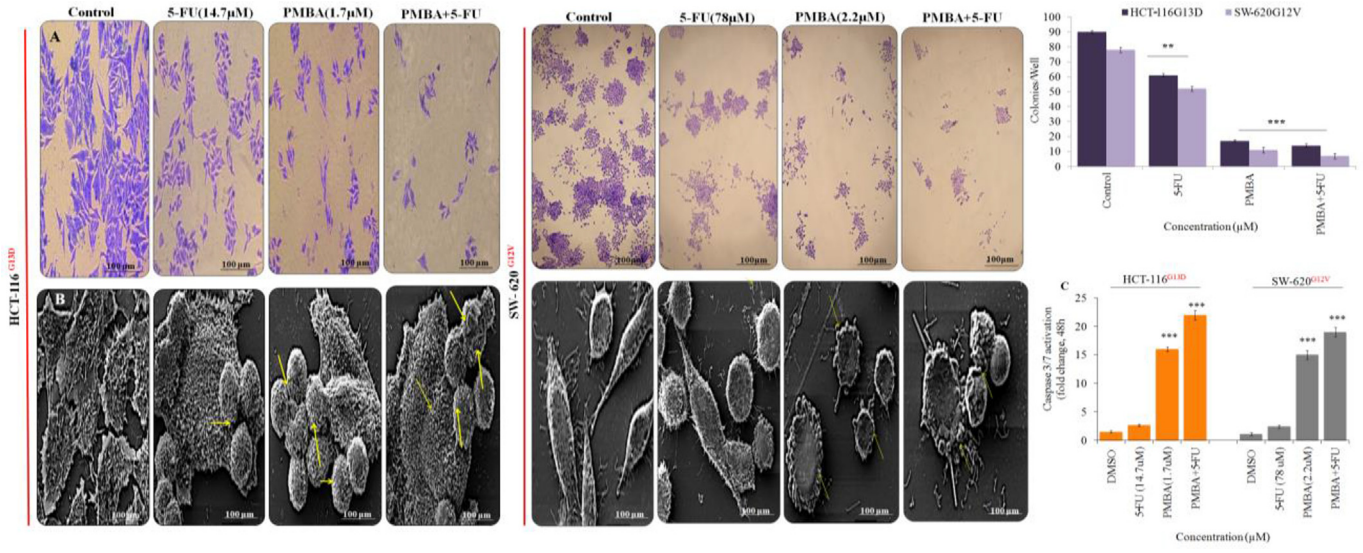

Figure 1. Morphological and Phenotypic response of KRAS mutant colon cancer cells to inhibitor PMBA treatment in 2D culture. (A) Quantified images of PMBA inhibited colony formation in KRAS mutant CRC cells (HCT-116^{G13D} and SW-620^{G12V}), but showed no effect on KRAS wild-type CRC cells (HT-29) stained with crystal violet stain after a 10-day treatment with DMSO, PMBA, 5-FU or both for 48 h n = 3, ns (non-significant); **P < 0.01; ***P < 0.001. (B) Representative scanning electron microscopy images of control and treated HCT-116^{G13D} and SW-620^{G12V} cells in 2D culture were shown. HCT-116^{G13D} and SW-620^{G12V} cells was grown as a monolayer (50,000 cells) for 24 h and further cultured in the presence or absence of PMBA, 5-FU or the combination (PMBA+5-FU) for 48 h. DMSO served as control. The arrow indicates the membrane blebbing, disappearance of microvilli and formation of apoptotic bodies in both the HCT-116^{G13D} and SW-620^{G12V} cells after treatment with PMBA alone and in combination. (C) HCT-116^{G13D} and SW-620^{G12V} cells were treated with the PMBA for 48 h at indicated concentrations and assayed by Caspase 3/7 activation kit in the regulation of apoptosis. n = 3, ns (non-significant); ***P < 0.001.

activated by PMBA. Whereas *in-vitro* colony assay was performed to measure the cell proliferation capability i.e. the ability of a single cell to grow into a colony. This assay tests each and every cell in the population for its ability to undergo unlimited divisions. HCT-116^{G13D} and SW-620^{G12V} cells were treated with different concentrations of PMBA, 5-FU and PMBA+5-FU at 1.7, 2.2 μM,14.7,78 μM and 1.7 + 14.7, 2.2 + 78 μM in which colonies were formed after 14 day treatment. It was found that PMBA significantly decreased colony formation in colon cancer cells (HCT-116^{G13D} and SW-620^{G12V} cells), but more proficient results were seen in combination of PMBA+5-FU as compared to the untreated control (A) (Figure 1A).

3.3. Assessment of DNA damage sensitivity in KRAS mutant cancer cells

PMBA induced comet formation for DNA nucleoids in the intact cells two KRAS mutant colon cancer cell lines, over a dose range of 1.7, 2.2, 14.7 and 78 μM for 48 h in both the cell lines. The plots revealed clear dose-response exhibiting ~2–17 fold for HCT-116^{G13D} and SW-620^{G12V} with higher measures of comet formation respectively, compared with the corresponding intact normal cells (HEK 293). In addition, for each cell line, the relative level of comet formation sustained the same array as varied in the intact normal cell line which exhibited a relatively low measure of comet formation at low dose but relatively greater measures at higher doses of combination (28.5 and 70 μM) (Figure 2, Table 1) (***$p < 0.001$).

3.4. Combination drug screen act as sensitizers to 5-FU

To inspect the therapeutic potentiality and estimate the reciprocity of *in-vitro* to *in-vivo* data for speculating sensitivity to treat KRAS mutant colorectal cancer, combination studies were conducted with 5-FU in HT-29, HCT-116 and SW-620 colorectal cancer cell lines, which carries a wild type and an activating KRAS mutation (G13D and G12V) (Figure 3A). The result of combination dose-response screen of PMBA and 5-FU, which was accomplished in HT-29^{WT}, HCT-116^{G13D} and SW-620^{G12V} cells assessed both single-combined agent activity and evaluated additive, synergistic, or antagonistic interactions over an array of doses (Figure 3B). As single agents, both PMBA and 5-FU revealed dose-dependent anti-proliferative activity with IC_{50} values of 1.7 and 2.2 μmol/L for 48 h respectively. A heat map of the expected response revealed multiplicative effect, as the two drugs act independently excess over single agent depicting the doses at which the drug combinations achieve better than predicted inhibition of cell viability (Figure 3C). The combination of PMBA and 5-FU was synergistic over the majority of dose-combinations studied. Accordant with the Bliss method, we discovered synergy at the majority of doses tested and importantly at doses that are thought to be clinically pertinent (Figure 3C). Subsequently, *in-vivo* evaluation extended further evidence that this drug combination generated a higher degree of antitumor activity than that achievable from single-agent treatment due to improved absorption of 5-FU administered with PMBA (Figure 3D).

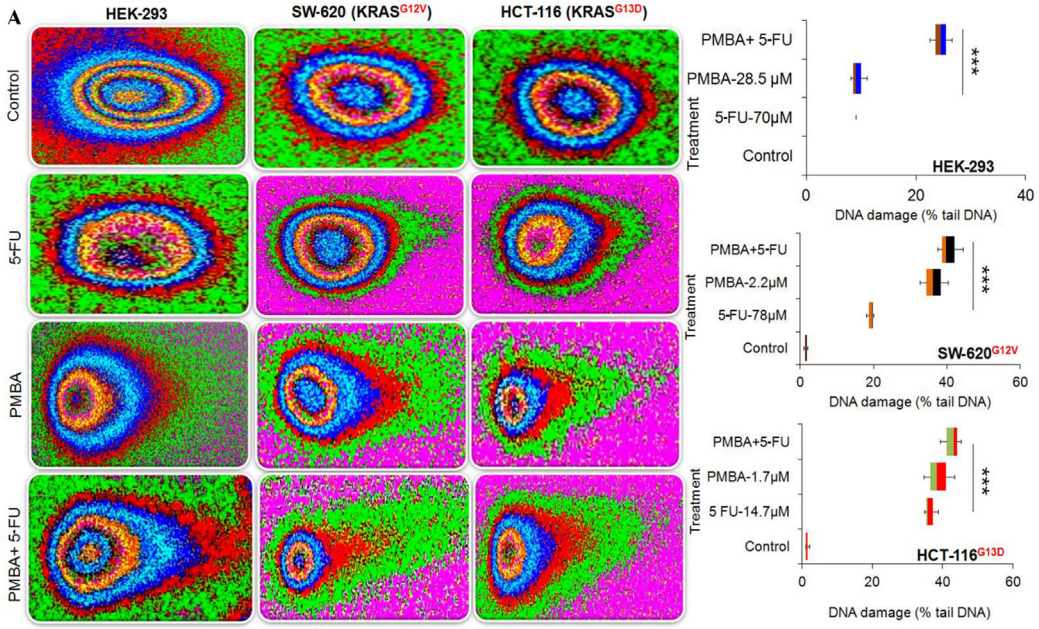

(B) Table 1	Head DNA		Tail DNA			Olive Tail Movement			Tail Length		
HCT-116^{G13D}	SW-620^{G12V}	HEK-293	HCT-116^{G13D}	SW-620^{G12V}	HEK-293	HCT-116^{G13D}	SW-620^{G12V}	HEK-293	HCT-116^{G13D}	SW-620^{G12V}	HEK-293
100	100	100	0	0	0	0	0	0	0	0	0
82.92±0.49	93.04±2.40	0	17±0.57	7±0.53	0	5.74±0.57	0	0	37.85±0.75	0	0
60.96±1.053	62.6±1.85	80.89±1.22	39.19±0.82	37.43±0.52	19±0.57	15.5±0.36	14.41±0.35	3.86±0.59	109±0.81	85.05±0.55	15.42±0.22
55.82±0.97	53.85±0.65	75.96±1.09	44.18±0.49	46.4±1.44	24±1.0	18.13±0.17	15.29±2.06	10.23±0.41	71.03±1.16	76.64±0.57	71.03±0.98

Figure 2. Comet DNA damage detection assay to directly examine whether activation of KRAS would result in decreased DNA damage. (A) KRAS$^{G13D,\ G12V}$ mutant cell lines after treatment with PMBA (1.7/2.2 μM)/5-FU (14.7/78 μM) combination therapy for 48 h. DNA damage was quantified via % DNA in tails. Each data point represents induction of mutant KRAS rendered cells resistant to PMBA-induced DNA damage, as indicated by the increased accumulation of DNA in tails with considerable strand breakage on chromosomal DNA and led to the appearance of an obscure halo around the nucleus of the HCT-116^{G13D} and SW-620^{G12V} cells. Combined treatment with PMBA and 5-FU as evidenced by an increased comet formation further. In contrast, PMBA had modest effects on HEK 293 cells, consistent with combination effects. Comet images (200X) in alkaline gel electrophoresis with HCT-116^{G13D} and SW-620^{G12V}cells were taken under an Olympus fluorescence microscope with an excitation filter (510 nm) and a barrier filter (590 nm) by using EtBr staining. Percentage of comet-positive cells is presented as the Mean ± SEM. Box indicates Mean ± SEM for each cell line, small square within the box indicates mean, and the horizontal bars indicate maximum and minimum values; n = 3 for each cell line denoting the % tail DNA damage. (B) Analysis and quantification of DNA damage as measured by comet assay in HCT 116^{G13D}, SW 620^{G12V} and HEK 293 cells treated with PMBA, 5-FU or both.

A

HCT-116^{G13D}			
5-FU(μM)	PMBA(μM)	CI	Mode
1.83	0.212	0.73	+
3.67	0.425	0.83	+
7.35	0.85	0.70	+
14.7	1.7	0.69	+
29.4	3.4	0.35	++
58.8	6.8	0.70	+
117.6	13.6	1.40	–

SW-620^{G12V}			
5-FU(μM)	PMBA(μM)	CI	Mode
9.75	0.275	0.74	+
19.5	0.55	0.88	+
39	1.1	0.81	+
78	2.2	0.78	+
156	4.4	0.43	++
312	8.8	0.86	+
624	17.6	1.72	-

HT-29^{WT}			
5-FU(μM)	PMBA(μM)	CI	Mode
10.25	3.25	1.08	-
20.5	6.5	1.00	-
41	13	1.30	-
82	26	1.13	-
164	52	1.15	-
328	104	0.64	+
625	208	1.29	-

PMBA:5-FU				
Cell Line	ED_{50}	ED_{75}	ED_{90}	Pearson, r
HCT-116^{G13D}	0.68	0.69	0.71	0.94
SW-620^{G12V}	0.73	0.77	0.82	0.90
HT-29^{WT}	1.06	1.04	1.01	0.89

B

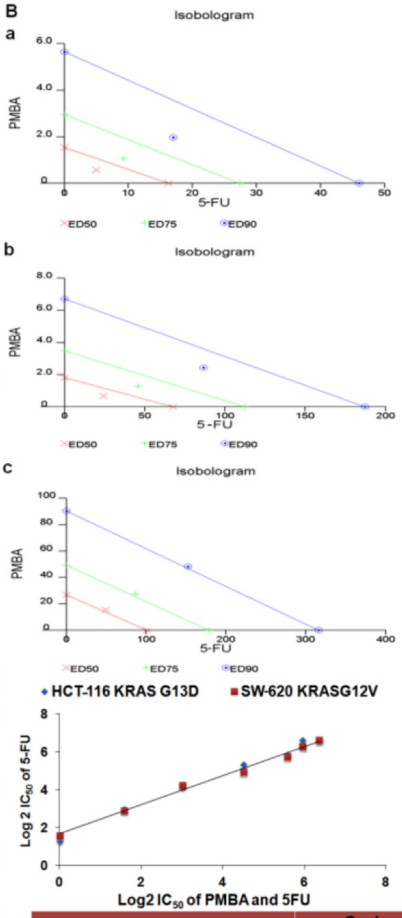

C

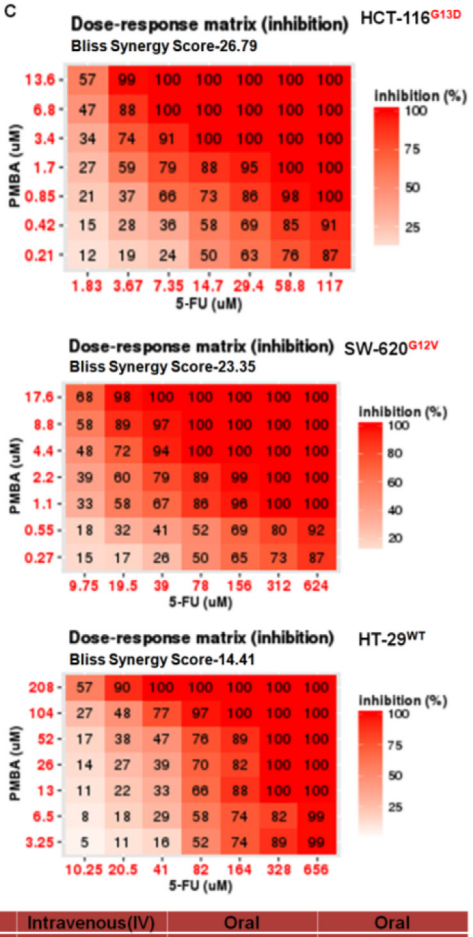

D

Pharmacokinetic parameter	Oral PMBA (20mg)	Intravenous(IV) PMBA (5mg)	Oral 5-FU (40mg)	Oral PMBA+5-FU
Cmax (ng/ml)	2555.8	-	2446.54	251.19
C0 (ng/ml)	-	32904.2	0	-
Tmax (h)	2.0	-	-	-
T1/2 (h)	**4.39**	**11.96**	**1.1**	**8.5**
AUC0-t (ng.h/ml)	21910.5	75646.9	1109.89	1644.35
AUC0-∞ (ng.h/ml)	22372.3	84360.8	1136.63	3470.04
Vd (l/kg)	5.66	1.02	56.32	70.85
Cl(l/h/kg)	0.89	0.06	35.19	5.76

Figure 3. Determination of synergistic combination of PMBA with 5-FU. (A) Combining PMBA with 5-FU inhibitor results in synergistic growth inhibition in KRAS-mutant colon cancer cell lines as calculated through Calcusyn version 2.1 and Synergy finder. The synergistic interaction between PMBA and 5-FU (validation screen) were examined across HT-29^{WT}, HCT-116^{G13D} and SW-620^{G12V} cell lines and correlated (Pearson correlation, R) with the synergy scores obtained in the initial screen treated with indicated concentration pairs of PMBA, 5-FU and with the combination of both. (B) Combination index (CI) at ED50, ED75, and ED90 values of PMBA with drug (5-FU) combination on two KRAS mutant colon cancer cell lines. The CI values at a Fa value of 0.5, 0.75, and 0.90 for isobologram were calculated with the Calcusyn version 2.1. Isobolograms of the combination of PMBA and 5-FU (a, b and c), Analysis of the combination of PMBA and 5-FU in (a) HCT-116 cells with a fixed ratio 1:8.63 of 5-FU: PMBA; (b) SW-620 cells with a fixed ratio of 1:35.4 of 5-FU: PMBA; (c) HT-29 cells with a fixed ratio of 1:3.15 of 5-FU: PMBA. The individual doses of PMBA and 5-FU, used to achieve 90% (straight line) growth inhibition (Fa = 0.90), 75% (hyphenated line) growth inhibition (Fa = 0.75), and 50% growth inhibition (Fa = 0.50) were plotted on the x- and y-axes. Combination index (CI) values is represented by points above (indicating-antagonism between drugs) or below the lines (indicating–synergy). X symbol ED50, plus sign ED75 and (open dotted circle) ED90 (monotherapy PMBA versus combination (CI $_{(5\text{-FU: (PMBA)})}$). CI*(combination index) obtained from the Fa value which denotes the fraction affected (e.g., Fa of 0.5 is equivalent to a reduction in cell growth). The CI value 1 shows synergism, = 1 show an additive while 1 shows antagonism. ++ Strong synergism, + synergism, -antagonism. (C) Heat maps encode synergistic effects induced by PMBA and 5-FU on HCT-116^{G13D} and SW-620^{G12V}cell lines. Cell lines were arranged into synergistic (red) and non-synergistic (green) by hierarchical clustering of expression signatures. Based on the activity, an expected GIC_{50} curve was inferred in which dose-response curves (logistic interpolation) of PMBA at a fixed concentration of 5-FU were compared. *P < 0.05; **P < 0.01. Comparison of Bliss synergy scores for the combination of PMBA and 5-FU with HT-29^{WT}, HCT-116^{G13D} and SW-620^{G12V}.Visualization of the dose–response matrix and the plots of phenotypic responses for the single drugs. (D) Pharmacokinetics study was carried out through oral administration of alone and combination of PMBA and 5-FU at a dose of 20 and 40 mg/kg in Balb/c mice respectively.

3.5. Influence of oncogenic KRAS mutation on CSC characteristics of colon cancer cells

The ability to form colonospheres was found to be ~3.5 fold for HCT-116^{G13D} and ~9 fold for SW-620 ^{G12V}cells, and was suggestive of a large intrinsic CSC population in both of the parental cell lines. Both CSC and parental cell lines showed varied expression of CD166, CD44 and EpCAM (Figure 4). SW-620-P and HCT-116-P cells had low expression of CD166, CD44 and EpCAM, which was increased in SW-620^{G12V}–CSCs and HCT-116^{G13D}-CSCs. The fold change between CSCs and parental cells was evaluated reciprocal to the expression of the housekeeping gene GAPDH. SW-620^{G12V}–CSCs and HCT-116^{G13D}-CSCs had a mean of 3.25 and 6.19, 11.2 and 27.5, 17.2 and 11.23 (***p < 0.001) with 6 and 7.7, 5.6 and 17, 19 and 8.6 fold increase in the expression of CD166, CD44 and EpCAM

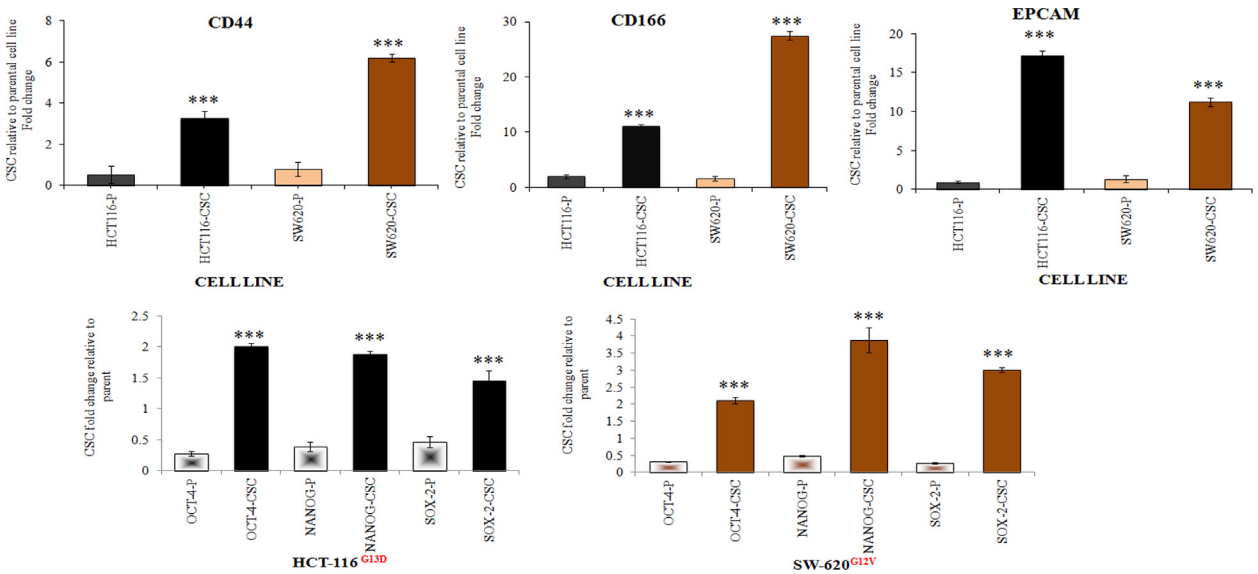

Figure 4. Quantitative Real-Time PCR was performed to reveal the expression of chemo-resistance proteins and CSC related markers in KRAS mutant colon cancer cell lines. Categorical expression of CSC markers-CD44, CD166, EpCAM and OCT-4, SOX-2, NANOG was evaluated in HCT-116^{G13D}, SW-620^{G12V} colonospheres and parental cells by qRT-PCR normalized to the expression of GAPDH. The mean fold change in gene expression±SEM is shown for the CSC cell lines relative to their respective parental cell lines (n = 3).

gene expression compared to respective parental cell lines: HCT-116-P and SW-620-P cells which had a mean of 0.52 and 0.8, 2 and 1.6, 0.9 and 1.3 [24,25]. Whereas expression of OCT-4, SOX-2, NANOG in parental HCT-116^{G13D} cell line was found to be 0.22, 0.35 and 0.3 with increase in expression of 10, 3.15 and 4.84 fold with mean of 1.94, 1.65 and 2. Also, in SW-620^{G12V}, the expression in parental cell line was 0.3, 0.27 and 0.48 as upon treatment there was increase in expression up to 7, 8 and 11-fold with mean of 2.11, 3.01 and 3.89, respectively.

3.6. Colonospheres have higher expression of drug resistance related genes

Expression of ABCC1 and ABCB1was significantly higher (~2.6 and 4, ~18.5 and 31-fold) in HCT-116 ^{G13D} and SW-620^{G12V}–CSCs compared to HCT116^{G13D} and SW-620^{G12V}–P cells (**p ≤ 0.01, ***p ≤ 0.001) with no change in ABCC1 or ABCG2 expression. SW620–CSCs had the highest expression of ABCB1 among the cell lines tested, whereas ABCC1 was expressed at low to moderate levels in all cell lines tested. These results support the increased expression of ABCB1 and ABCG2 in CSCs. The gene expression of ALDH1A1, ALDH1A2, ALDH1A3 and ALDH3A1 was also examined using qRT-PCR (Nolan et al., 2006). Both parental and CSC enriched cell lines had a low expression of ALDH1A2. ALDH1A3 and ALDH3A1, while it was moderate in both HCT-116^{G13D}-and SW-620^{G12V} –CSCs with no significant differences expression between parental cell lines, but HCT-116^{G13D}-and SW620^{G12V}–CSCs had significantly higher expression of ALDH1A1 (***p ≤ 0.001,**p ≤ 0.01) (Figure 5).

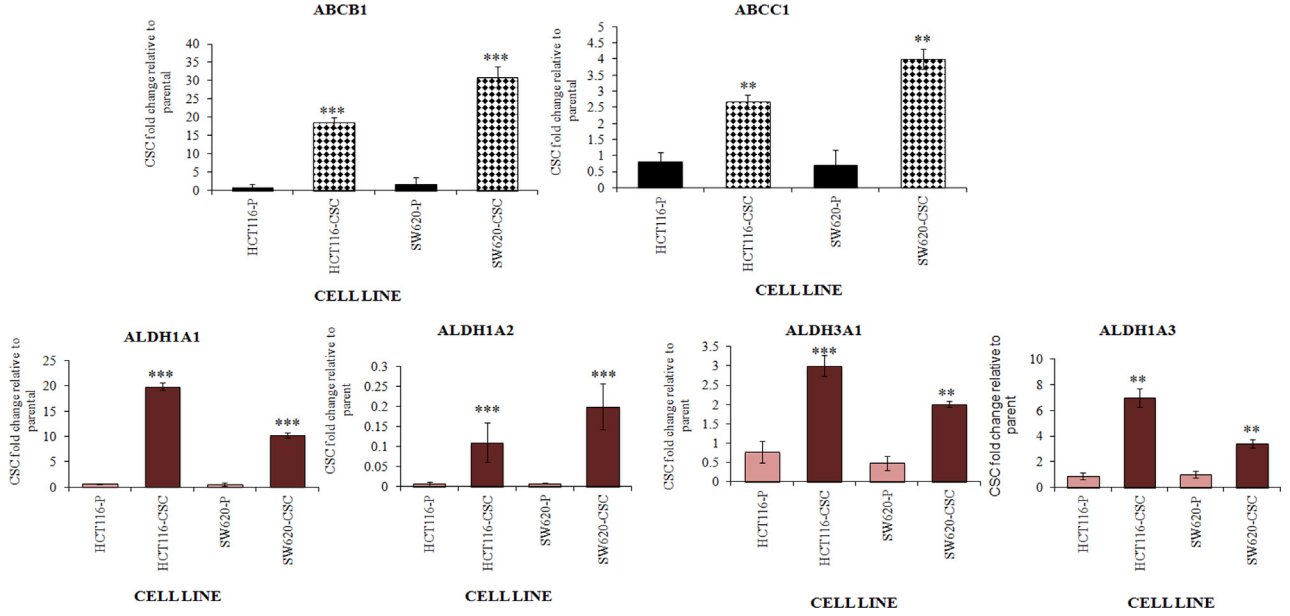

Figure 5. Expression analysis of Drug resistance and CSC markers in HCT 116^{G13D} and SW 620^{G12V} cells. (A9) Gene expression analysis of ABC transporter family members: ABCB1, ABCC1 and ALDH1A1, ALDH1A2, ALDH1A3, ALDH3A1 was quantified in CSCs and parental cells. Target gene expression was normalized to the expression of the reference gene, GAPDH. The mean fold change in gene expression ±SEM is shown for the CSC cell lines relative to their respective parental cell lines (n = 3).

3.7. Evaluation of 3D colonospheres chemotherapy treatment in response to PMBA and 5-FU

After ten days of growth, parental and CSC derived colonospheres were treated with 5-FU (14.7/78 μM) and PMBA (1.7/2.2 μM). HCT-116^{G13D} parental derived colonospheres were sensitive to treatment with PMBA (***p ≤ 0.001) and 5-FU. A reduction in metabolically active cells was accompanied by visible colonosphere dissociation. SW-620^{G12V}-CSC and HCT-116^{G13D}-CSCs derived colonospheres were resistant to 5-FU treatment (*p ≤ 0.05) even with prolonged exposure (Figure 6). Colonospheres were also treated with PMBA, 5-FU or both, at doses lower and higher than the IC_{50} values and dissociation was seen in response to high doses of chemotherapy with prolonged exposure. Expressional analysis of c-Kit through western blotting revealed its role in modulating the tumor initiating colon stem cells through its activation of RAS pathway and treatment with both PMBA alone or in combination resulted its suppression.

3.8. Drug resistance related gene expression changes following chemotherapy treatment

Parental monolayer cells, and CSC colonospheres were treated with 5-FU (14.7/78 μM), PMBA (1.7/2.2 μM) or both for 48 h and qRT-PCR

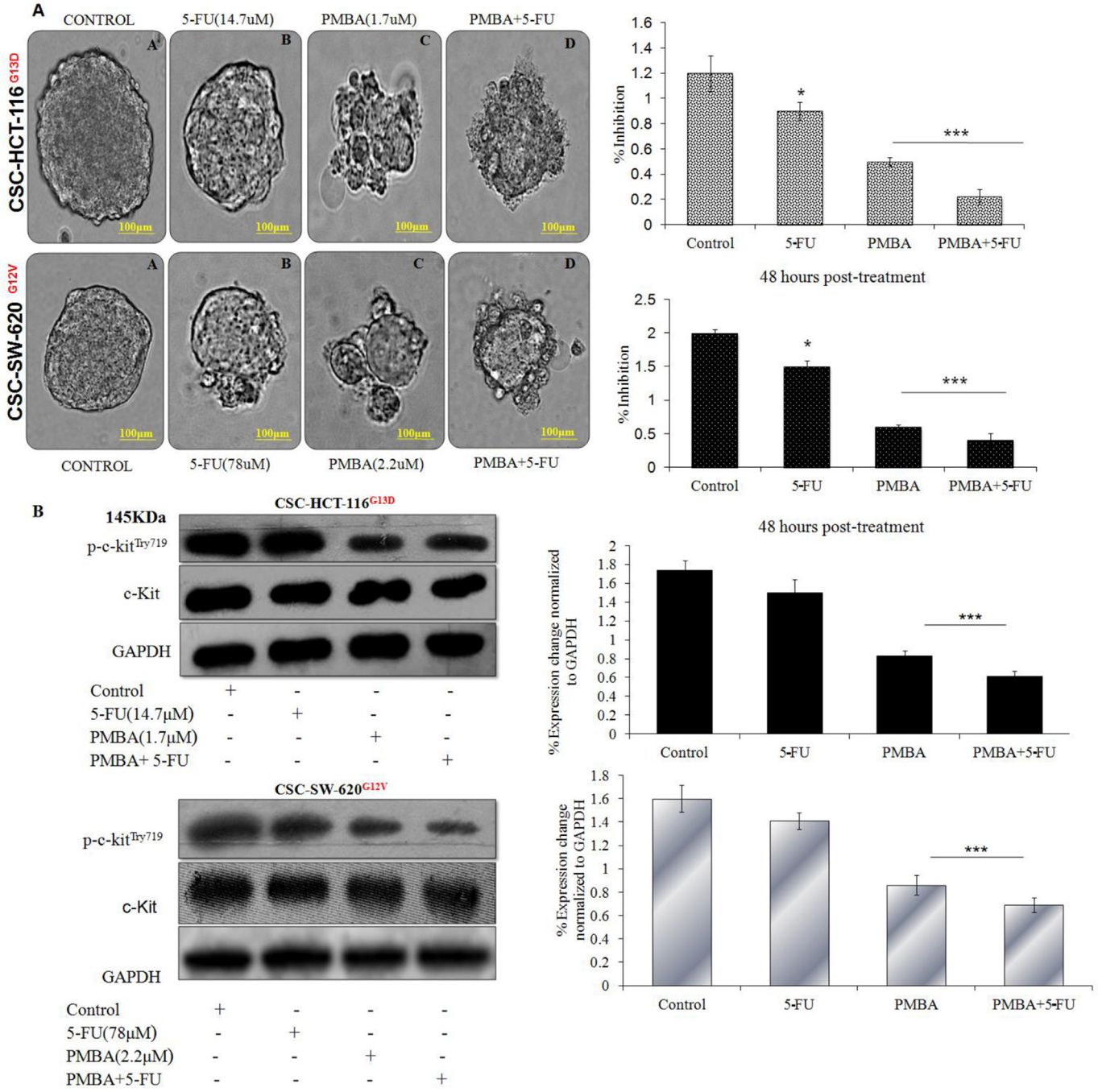

Figure 6. Impact of PMBA, 5-FU or both in Pluripotent transcription factors, ABC transporter and ALDH gene expression. (A) KRAS-driven colon cancer cell proliferation in 3D culture: Phase-contrast images of HCT-116^{G13D} and SW-620^{G12V} colonospheres at 48 h following EGF stimulation (10 ng/mL) following chemotherapy treatment against PMBA (1.7, 2 μM/mL), 5-FU (14.7,78 μM/mL), or the combination. Mean ± SEM number of dispersed cells per colonospheres from triplicate shown (*P < 0.05, ***P < 0.001). (B) c-Kit expression analysed by western blotting in both CSC-SW-620 and CSC-HCT-116 and markedly decreased in expression with treatment with PMBA and PMBA+5-FU as compared to 5-FU alone (ns-non-significant, ***P < 0.001).

analysis was done to determine the gene expression levels of ABCB1, ABCC1, ALDH1A1, ALDH1A3 and ALDH3A1 as compared to control (untreated) samples. Treatment with 5-FU did not alter the expression of these genes in any of the cell lines tested. Both ABCB1 and ABCC1expression was ~4 and 2-fold down regulated in HCT-116^{G13D}- and SW-620^{G12V}–CSCs in response to PMBA and both (PMBA+ 5-FU) (***p ≤ 0.001) (Figure 7A). Also, increased in response to treatment, ALDH1A1, ALDH1A3 and ALDH3A1 expression was lower than levels detected in respective untreated CSCs (**p ≤ 0.01) (Figure 7B). The expression of stem cell transcriptional factor such as OCT-4, NANOG and SOX-2 (Figure 7C) also found to be down regulated by treatment with PMBA alone or both PMBA+5-FU. Collectively, these results provide evidence that chemotherapy treatment reduces the expression of drug-resistance associated genes in both CSC.

3.9. Pharmacokinetics of PMBA, 5-FU and PMBA+5-FU

Pharmacokinetics studies were carried out following oral (PO) and intravenous (IV) administration of PMBA at a single dose of 20 mg/kg, 5 mg/kg and 40 mg for 5-FU, whereas in combination of PMBA and 5-FU in Balb/c mice. Mean plasma concentration versus time profiles of PMBA, 5-FU and PMBA+5-FU with pharmacokinetic parameters of PMBA, 5-FU and PMBA+5-FU are represented in Tables 2 and 3, respectively. C_{max} of PMBA was achieved after 2 h of orally dose administration. The half-life of the molecule was excellent for both the routes of administration. Excellent AUCs of the candidate were obtained through IV route in comparison to oral route. Slow clearance of the molecule after IV administration was seen in comparison to the oral administration. Oral exposure of the compound can be improved by approaching various application of the formulation. Moreover, oral exposure of the candidate is acceptable based on its proposed therapeutic application, and a number of drugs available in the market have a similar type of exposure profile. Overall, PMBA has satisfactory pharmacokinetic profile route that insinuates further development. Furthermore, Pharmacokinetics study was carried out following oral administration of combination of PMBA and 5-FU at a dose of 20 and 40 mg/kg in Balb/c mice respectively. Also, Time vs. plasma concentration profile of both PMBA and 5-FU was depicted in Table 3. It was observed that PMBA and 5-FU was absorbed rapidly as time to reach maximum plasma concentration (T_{max}) after dose administration was only 30 min. $T_{1/2}$ was increased up to 7.7-fold when given PMBA with 5-FU as compared to 5-FU alone. Plasma half-life ($T_{1/2}$) of PMBA in combination therapy was found to be excellent as $T_{1/2}$ more than 2 h is sufficient for a new chemical entity to proceed for further clinical research.

4. Discussion

5-FU, a water-soluble anti-metabolite, is being used as a chemotherapeutic and neoplastic agent in treating colon cancers. On a clinical scale it has, however, shown considerable limitations owing to its low bioavailability and attained drug resistance (Christensen e al., 2019). In advanced CRC, the curative accountability of 5-FU is less than 10–15%. In order to achieve a better therapeutic effect, with fewer side effects, various 5-FU combination and formulation strategies have been

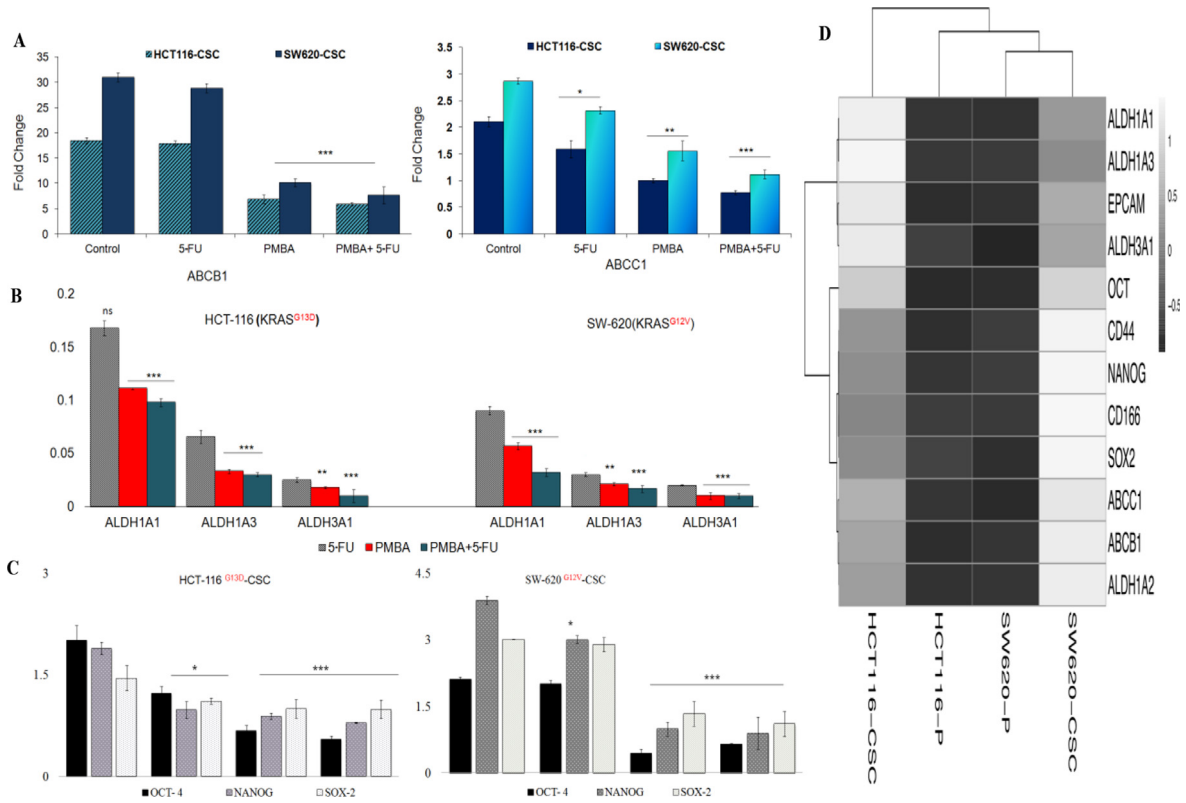

Figure 7. (A) Expression of ABCB1 and ABCC1in CSC-HCT-116 and SW-620 cells were found to be up-regulated but PMBA alone and in combination with 5-FU down-regulated its expression effectively in comparison to 5-FU (*P < 0.05; **P < 0.01; ***P < 0.001). (B) Expression comprises of ALDH1A1, ALDH1A3 and ALDH3A1 was increased in HCT-116^{G13D} and SW-620^{G12V} cell lines imparting resistance to chemotherapeutic drugs. Treatment involving PMBA and PMBA+ 5-FU resulted reduced expression when compared with 5-FU (ns-non-significant, **P < 0.01; ***P < 0.001). (C) HCT-116^{G13D} and SW-620^{G12V}cells treated with 5-FU (14.7, 78 μM), PMBA (1.7, 2.2 μM) or both for 48 h and normalized to the expression of GAPDH with changes seen in gene expression of pluripotent transcription factors (OCT-4, NANOG and SOX-2), ABC transporter and ALDH variant in CSC and parental cells quantified using RT-qPCR. Results are Mean ± SEM (n = 3). *P < 0.05; **P < 0.01; ***P < 0.001; ns-non-significant. (D) Heatmap and unsupervised hierarchical clustering analysis of mRNA expression in HCT-116^{G13D} and SW-620^{G12V}–P and CSC cell-associated with a variable expression as shown compared to control; red is up-regulated, and green is down-regulated compared to the mean of the individual gene's expression levels (ClustVis).

Table 2. Pharmacokinetic parameters of PMBA after oral and IV administration in Balb/c mice.

Pharmacokinetic Parameters	Oral	IV
C_{max} (ng/ml)	2555.8	-
C_0 (ng/ml)	-	32904.2
T_{max} (h)	2.0	-
$T_{1/2}$ (h)	4.39	11.96
AUC_{0-t} (ng.h/ml)	21910.5	75646.9
$AUC_{0-\infty}$ (ng.h/ml)	22372.3	84360.8
V_d (l/kg)	5.66	1.02
Cl (l/h/kg)	0.89	0.06

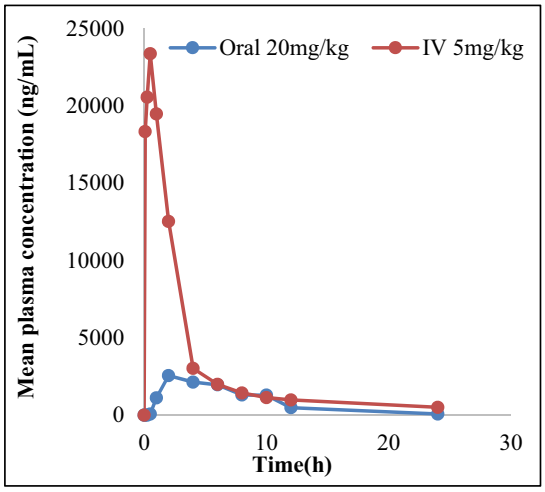

discovered aiming to overcome its short half-life, poor efficacy, low bioavailability and higher toxicity. The inefficient selectivity of 5-FU for cancerous cells limits its effectiveness in cancer chemotherapy in achieving a proficient effect. Many combination approaches have been coming forward to overcome these disadvantages of 5-FU in CRC therapy (Afrin et al., 2018, 2021). 5-FU is an analogue of the pyrimidine nucleobase uracil which can enter the cells *via* facilitated transport mechanism. 5-FU is metabolized into fluorodeoxyuridine monophosphate (FdUMP), fluorodeoxyuridine triphosphate (FdUTP) and fluorouridine triphosphate (FUTP) which prevent the synthesis of RNA and thymidylate synthase (TS) activity in cancerous cells. On the 5-FU catabolism, a rate-limiting enzyme dihydropyrimidine dehydrogenase (DPD) is catabolized to dihydrofluorouracil (DHFU) and the level is found to be increased in tumor cells. Mostly, the up-regulation of

Table 3. Pharmacokinetic parameters of 5-FU, PMBA+5-FU after oral administration in Balb/c mice.

Pharmacokinetic Parameters	5-FU	PMBA+5-FU
$T_{1/2}$ (h)	1.1	8.5
C_{max} (ng/mL)	2446.54	251.19
C_0 (ng/mL)	0	-
AUC_{0-t} (ng·h/mL)	1109.89	1644.35
$AUC_{0-\infty}$ (ng·h/mL)	1136.63	3470.04
CL (mL/min/kg)	35.19	5.76
V_d (L/kg)	56.32	70.85
V_{ss} (L/kg)	Not done	Not done
Time points considered for T1/2 calculation:	1 - 4h	4-10 h

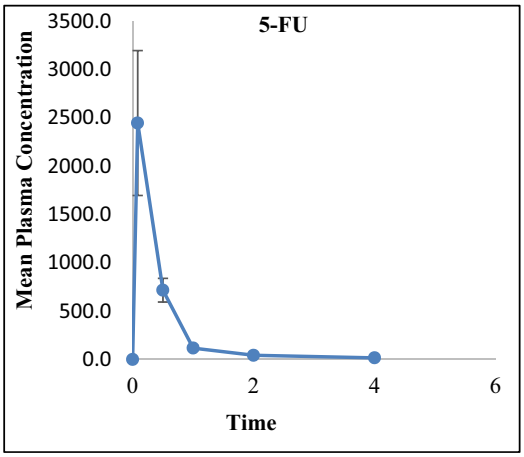

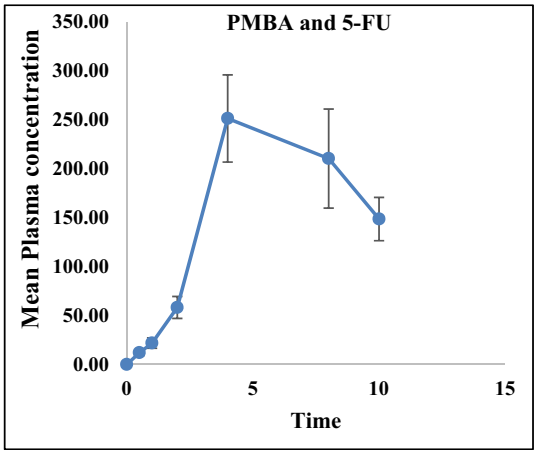

dihydropyrimidine dehydrogenase (DPD) gene expression in CRC is associated with 5-FU acquired drug resistance (ADR) (Zhang et al., 2008).

Potential regimes are coming along to enhance chemotherapy by 5-FU and one of the most important objectives of pharmaceutical research is to discover novel 5-FU combinations to minimize side effects with improved clinical efficacy. Furthermore, combining nutraceuticals therapeutic agents with standard 5-FU to enhance its therapeutic efficacy is another beneficial potential of these drug delivery systems for the treatment of CRC which can also enhance the sensitivity of tumor cells to 5-FU, so as to overcome drug resistance (Almahdi et al., 2020). A distinguished sensitivity to KRAS inhibition (*in vitro*) with PMBA in cancer cell lines has been established and also confirmed by culture reliant effect of KRAS expression over monolayer *versus* 3D-colon spheroids (Sun et al., 2017; Selby et al., 2017). The extension of these KRAS-dependency correlations to the *in-vivo* environment from the breakthrough that PMBA is highly efficacious in mono- and combination-studies in several cancer cell lines highlighted its basic importance of mutant KRAS driving cancer augmentation and mortality *in-vivo*. Moreover, these findings not only implicated that 3D-colon spheroid cultures better speculate the *in-vivo* sensitivity of KRAS mutant cancer cells to PMBA, but also promoted that *in-vitro* studies determining KRAS dependency using adherent monolayer cell cultures significantly minimize KRAS peripheral action *in-vivo* (Fujita-Sato et al., 2015). The 3D cultures are becoming more frequently recognized and utilized to better imitate the *in-vivo* environment and response to chemotherapy with additional therapeutic targets (e.g., HER2 and EGFR) (Ekert et al., 2014; Howes et al., 2014). We are not apprised of any approved oncology drug that exhibits distinctive activity between 2D and 3D cultures as considerable as KRAS inhibition. This has phenomenal translational inference for interpreting *in-vitro* synthetic lethal association of KRAS as a navigating oncogene. In future clinical assessment to a $KRAS^{G13D,\ G12V}$ mutated patient; 3D cultures will prove to be an eminent screen. Further, targeting drug resistance genes (ABCB1, ABCC1, ALDH1A1, ALDH1A3 and ALDH3A1) in 3D population of colon cancer cell lines carrying KRAS wild type and mutant profile evaluated the PMBA and 5-FU combinations (Huang et al., 2009; Vasiliou et al., 2004). This indicated enhanced efficacy in the activity of 5-FU when combined with PMBA, and accomplished the drug design for β-BA combinatorial targeted therapy impacting KRAS mutant colon cancer cells with transmuted expression of gene complexes in processes like apoptosis, cell cycle progression and relocation, which were doubtlessly the out turn of disordered cellular metabolism, growth, and redox balance.

Collectively, the *in-vivo* results confirmed that PMBA is broadly efficacious as a single and combination agent throughout colorectal model and provided evidence that a significant portion of patients with $KRAS^{G13D,\ G12V}$ mutations would get assistance from KRAS directed therapies. It is fortuitous to consider that PK profile for PMBA (20 mg) and PMBA+5-FU (20 + 40 mg) enabled maximum target tenancy with the inherent good chemical and metabolic stability for an increased stretch of time at the doses employed and sufficient to achieve a therapeutic efficacy in the tumor model in mono as well as combination therapy. This is the first study that demonstrated the effectiveness of PMBA in combination with 5-FU against KRAS mutant colon cancer. In this study, we demonstrated that PMBA and 5-FU inhibited $HCT\text{-}116^{G13D}$ and $SW\text{-}620^{G12V}$ KRAS mutant colon cancer cells proliferation (*in-vitro*) with IC_{50} value of 1.7 μM/mL, 2.2 μM/mL and HT-29 cells with 25.89 μg/mL. In our previous study, PMBA was found to be more potent and selective when compared with the IC_{50} observed with AKBA treatment in other cancer cell lines (Kumar et al., 2016). The anti-proliferative potential of PMBA on different cancer cell lines has been found to vary, based on sensitivity and type of cancer. This study has been conducted on $HCT\text{-}116^{G13D}$, $SW\text{-}620^{G12V}$ and $HT\text{-}29^{WT}$ cell lines in order to determine interaction pattern and the efficacy between PMBA and 5-FU by using Isobologram analysis to assess the qualitative as well as quantitative measure of nature and interaction range between two anti-tumor agents. Further, SynergyFinder R implemented algorithms to calculate the synergy scores for dose–response matrix data via Bliss model as a 2D and 3D synergy map over the dose matrix, revealed the expected response as a multiplicative effect as if the two drugs acted independently. In the present investigation, isobologram analysis of different KRAS cell lines exhibited that PMBA enhanced the cytotoxicity of 5-FU in both $HCT\text{-}116^{G13D}$, $SW\text{-}620^{G12V}$ cells (CI value ED50, ED75 and ED90 0.53–0.76) in a synergistic manner, whereas in HT-29 cells (CI value ED50, ED75 and ED90 0.55–0.79) it showed concentration additive behaviour. After determining the efficacy of PMBA alone and in combination with 5-FU on $HCT\text{-}116^{G13D}$, $SW\text{-}620^{G12V}$ cells and $HT\text{-}29^{WT}$ cells *in-vitro*, pharmacokinetics studies have been carried out to test the efficacy of PMBA against 5-FU in Swiss mice in which $T_{1/2}$ was increased by 7.7-fold when given PMBA with 5-FU as compared to 5-FU alone. Thus, it is imperative to design new combinatorial approaches with PMBA that allow dose reduction, enhance the drug effectiveness and reduce the toxicity.

Declarations

Author contribution statement

Arem Qayum: Conceived and designed the experiments; Performed the experiments; Analyzed and interpreted the data; Wrote the paper.

Asmita Magotra: Performed the experiments; Analyzed and interpreted the data.

Syed Mohmad Shah: Analyzed and interpreted the data.

Utpal Nandi; PR Sharma: Contributed reagents, materials, analysis tools or data.

Bhahwal Ali Shah: Contributed reagents, materials, analysis tools or data; Analyzed and interpreted the data.

Shashank Kumar Singh: Conceived and designed the experiments; Contributed reagents, materials, analysis tools or data.

Funding statement

This work was supported by the Council of Scientific and Industrial Research (CSIR), New Delhi, India CSIR project BSC-0205.

Data availability statement

Data included in article/supplementary material/referenced in article.

Declaration of interests statement

The authors declare no conflict of interest.

Additional information

No additional information is available for this paper.

References

Afrin, S., Giampieri, F., Forbes-Hernández, T.Y., Gasparrini, M., Amici, A., Cianciosi, D., Quiles, J.L., Battino, M., 2018. Manuka honey synergistically enhances the chemopreventive effect of 5-fluorouracil on human colon cancer cells by inducing oxidative stress and apoptosis, altering metabolic phenotypes and suppressing metastasis ability. Free Radic. Biol. Med. 126, 41–54.

Afrin, S., Giampieri, F., Cianciosi, D., Alvarez-Suarez, J.M., Bullon, B., Amici, A., Quiles, J.L., Forbes-Hernández, T.Y., Battino, M., 2021. Strawberry tree honey in combination with 5-fluorouracil enhances chemosensitivity in human colon adenocarcinoma cells. Food Chem. Toxicol. : Int. J. Publ. Br. Industr. Biol. Res. Asso. 156, 112484.

Bahmad, H.F., Cheaito, K., Chalhoub, R.M., Hadadeh, O., Monzer, A., Ballout, F., El-Hajj, A., Mukherji, D., Liu, Y.N., Daoud, G., Abou-Kheir, W., 2018. Sphere-formation assay: three-dimensional in vitro culturing of prostate cancer stem/progenitor sphere-forming cells. Front. Oncol. 8, 347.

Bayat Mokhtari, R., Homayouni, T.S., Baluch, N., Morgatskaya, E., Kumar, S., Das, B., Yeger, H., 2017. Combination therapy in combating cancer. Oncotarget 8 (23), 38022–38043.

Beretta, G.D., Petrelli, F., Stinco, S., Cabiddu, M., Ghilardi, M., Squadroni, M., Borgonovo, K., Barni, S., 2013. FOLFIRI + bevacizumab as second-line therapy for metastatic colorectal cancer pretreated with oxaliplatin: a pooled analysis of published trials. Med. Oncol. (Northwood, London, England) 30 (1), 486.

Bijnsdorp, I.V., Giovannetti, E., Peters, G.J., 2011. Analysis of drug interactions. Methods Mol. Biol. 731, 421–434.

Cassidy, J., Tabernero, J., Twelves, C., Brunet, R., Butts, C., Conroy, T., Debraud, F., Figer, A., Grossmann, J., Sawada, N., Schöffski, P., Sobrero, A., Van Cutsem, E., Díaz-Rubio, E., 2004. XELOX (capecitabine plus oxaliplatin): active first-line therapy for patients with metastatic colorectal cancer. J. Clin. Oncol. : Off. J. Am. Soc. Clin. Oncol. 22 (11), 2084–2091.

Chou, T.C., 2010. Drug combination studies and their synergy quantification using the Chou-Talalay method. Cancer Res. 70 (2), 440–446.

Christensen, S., Van der Roest, B., Besselink, N., Janssen, R., Boymans, S., Martens, J., Yaspo, M.L., Priestley, P., Kuijk, E., Cuppen, E., Van Hoeck, A., 2019. 5-Fluorouracil treatment induces characteristic T>G mutations in human cancer. Nat. Commun. 10 (1), 4571.

Chu, P., Clanton, D.J., Snipas, T.S., Lee, J., Mitchell, E., Nguyen, M.L., Hare, E., Peach, R.J., 2009. Characterization of a subpopulation of colon cancer cells with stem cell-like properties. Int. J. Cancer 124 (6), 1312–1321.

Crowley, L.C., Christensen, M.E., Waterhouse, N.J., 2016. Measuring survival of adherent cells with the colony-forming assay. Cold Spring Harb. Protoc. 2016 (8).

de Gramont, A., Figer, A., Seymour, M., Homerin, M., Hmissi, A., Cassidy, J., Boni, C., Cortes-Funes, H., Cervantes, A., Freyer, G., Papamichael, D., Le Bail, N., Louvet, C., Hendler, D., de Braud, F., Wilson, C., Morvan, F., Bonetti, A., 2000. Leucovorin and fluorouracil with or without oxaliplatin as first-line treatment in advanced colorectal cancer. J. Clin. Oncol. : Off. J. Am. Soc. Clin. Oncol. 18 (16), 2938–2947.

Delord, J.P., Pierga, J.Y., Dieras, V., Bertheault-Cvitkovic, F., Turpin, F.L., Lokiec, F., Lochon, I., Chatelut, E., Canal, P., Guimbaud, R., Mery-Mignard, D., Cornen, X., Mouri, Z., Bugat, R., 2005. A phase I clinical and pharmacokinetic study of capecitabine (Xeloda) and irinotecan combination therapy (XELIRI) in patients with metastatic gastrointestinal tumours. Br. J. Cancer 92 (5), 820–826.

Dheer, D., Gupta, R., Singh, D., Magotra, A., Singh, G., Gupta, P.N., Shankar, R., 2019. Hyaluronic Acid-Tacrolimus Bioconjugate: synthesis, characterization and pharmacokinetic investigation of an acid-responsive macromolecular prodrug. ACS Appl. Bio Mater. 2 (11), 4728–4736.

Doroshow, J.H., Simon, R.M., 2017. On the design of combination cancer therapy. Cell 171 (7), 1476–1478.

Eberhard, D.A., Johnson, B.E., Amler, L.C., Goddard, A.D., Heldens, S.L., Herbst, R.S., Ince, W.L., Jänne, P.A., Januario, T., Johnson, D.H., Klein, P., Miller, V.A., Ostland, M.A., Ramies, D.A., Sebisanovic, D., Stinson, J.A., Zhang, Y.R., Seshagiri, S., Hillan, K.J., 2005. Mutations in the epidermal growth factor receptor and in KRAS are predictive and prognostic indicators in patients with non-small-cell lung cancer treated with chemotherapy alone and in combination with erlotinib. J. Clin. Oncol. : Off. J. Am. Soc. Clin. Oncol. 23 (25), 5900–5909.

Ekert, J.E., Johnson, K., Strake, B., Pardinas, J., Jarantow, S., Perkinson, R., Colter, D.C., 2014. Three-dimensional lung tumor microenvironment modulates therapeutic compound responsiveness in vitro–implication for drug development. PLoS One 9 (3), e92248.

Entezar-Almahdi, E., Mohammadi-Samani, S., Tayebi, L., Farjadian, F., 2020. Recent advances in designing 5-fluorouracil delivery systems: a stepping stone in the safe treatment of colorectal cancer. Int. J. Nanomed. 15, 5445–5458.

Fischer, E.R., Hansen, B.T., Nair, V., Hoyt, F.H., Dorward, D.W., 2012. Scanning electron microscopy. Curr. Prot. Microbiol. Chapter 2, Unit2B.2–2B.2.

Fujita-Sato, S., Galeas, J., Truitt, M., Pitt, C., Urisman, A., Bandyopadhyay, S., Ruggero, D., McCormick, F., 2015. Enhanced MET translation and signaling sustains K-Ras-Driven proliferation under anchorage-independent growth conditions. Cancer Res. 75 (14), 2851–2862.

Heinemann, V., von Weikersthal, L.F., Decker, T., Kiani, A., Kaiser, F., Al-Batran, S.E., Heintges, T., Lerchenmüller, C., Kahl, C., Seipelt, G., Kullmann, F., Moehler, M., Scheithauer, W., Held, S., Miller-Phillips, L., Modest, D.P., Jung, A., Kirchner, T., Stintzing, S., 2021. FOLFIRI plus cetuximab or bevacizumab for advanced colorectal cancer: final survival and per-protocol analysis of FIRE-3, a randomised clinical trial. Br. J. Cancer 124 (3), 587–594.

Howes, A.L., Richardson, R.D., Finlay, D., Vuori, K., 2014. 3-Dimensional culture systems for anti-cancer compound profiling and high-throughput screening reveal increases in EGFR inhibitor-mediated cytotoxicity compared to monolayer culture systems. PLoS One 9 (9), e108283.

Huang, E.H., Hynes, M.J., Zhang, T., Ginestier, C., Dontu, G., Appelman, H., Fields, J.Z., Wicha, M.S., Boman, B.M., 2009. Aldehyde dehydrogenase 1 is a marker for normal and malignant human colonic stem cells (SC) and tracks SC overpopulation during colon tumorigenesis. Cancer Res. 69 (8), 3382–3389.

Ianevski, A., He, L., Aittokallio, T., Tang, J., 2017. SynergyFinder: a web application for analyzing drug combination dose-response matrix data. Bioinformatics (Oxford, England) 33 (15), 2413–2415.

Kumar, A., Qayum, A., Sharma, P.R., Singh, S.K., Shah, B.A., 2016. Synthesis of β-boswellic acid derivatives as cytotoxic and apoptotic agents. Bioorg. Med. Chem. Lett. 26 (1), 76–81.

Lu, C.Y., Yeh, Y.S., Huang, C.W., Ma, C.J., Yu, F.J., Wang, J.Y., 2014. FOLFIRI and regorafenib combination therapy with dose escalation of irinotecan as fourth-line treatment for patients with metastatic colon cancer according to UGT1A1 genotyping. OncoTargets Ther. 7, 2143–2146.

Lu, Y., Liu, Y., Yang, C., 2017. Evaluating in vitro DNA damage using comet assay. J. Vis. Exper.: JoVE (128), 56450.

Magotra, A., Sharma, A., Singh, S., Ojha, P.K., Kumar, S., Bokolia, N., Wazir, P., Sharma, S., Khan, I.A., Singh, P.P., Vishwakarma, R.A., Singh, G., Nandi, U., 2018. Physicochemical, pharmacokinetic, efficacy and toxicity profiling of a potential nitrofuranyl methyl piperazine derivative IIIM-MCD-211 for oral tuberculosis therapy via in-silico-in-vitro-in-vivo approach. Pulm. Pharmacol. Therapeut. 48, 151–160.

Nolan, T., Hands, R.E., Bustin, S.A., 2006. Quantification of mRNA using real-time RT-PCR. Nat. Protoc. 1 (3), 1559–1582.

Osawa, H., Handa, N., Minakata, K., 2014. Efficacy and safety of capecitabine and oxaliplatin (CapOX) as an adjuvant therapy in Japanese for stage II/III colon cancer in a group at high risk of recurrence in retrospective study. Oncol. Res. 22 (5-6), 325–331.

Roberts, P.J., Der, C.J., 2007. Targeting the Raf-MEK-ERK mitogen-activated protein kinase cascade for the treatment of cancer. Oncogene 26 (22), 3291–3310.

Schultheis, B., Folprecht, G., Kuhlmann, J., Ehrenberg, R., Hacker, U.T., Köhne, C.H., Kornacker, M., Boix, O., Lettieri, J., Krauss, J., Fischer, R., Hamann, S., Strumberg, D., Mross, K.B., 2013. Regorafenib in combination with FOLFOX or FOLFIRI as first- or second-line treatment of colorectal cancer: results of a multicenter, phase Ib study. Ann. Oncol. : Off. J. Euro. Soc. Med. Oncol. 24 (6), 1560–1567.

Selby, M., Delosh, R., Laudeman, J., Ogle, C., Reinhart, R., Silvers, T., Lawrence, S., Kinders, R., Parchment, R., Teicher, B.A., Evans, D.M., 2017. 3D models of the NCI60 cell lines for screening oncology compounds. SLAS Discov.: Adv. Life Sci. R D 22 (5), 473–483.

Shaker, G.H., Melake, N.A., 2012. Use of the single cell gel electrophoresis (comet assay) for comparing apoptotic effect of conventional antibodies versus nanobodies. Saudi Pharmaceut. J. :SPJ:Off. Publ. Saudi Pharmaceut. Soc. 20 (3), 221–227.

Sun, C., Fang, Y., Yin, J., Chen, J., Ju, Z., Zhang, D., Chen, X., Vellano, C.P., Jeong, K.J., Ng, P.K., Eterovic, A., Bhola, N.H., Lu, Y., Westin, S.N., Grandis, J.R., Lin, S.Y., Scott, K.L., Peng, G., Brugge, J., Mills, G.B., 2017. Rational combination therapy with PARP and MEK inhibitors capitalizes on therapeutic liabilities in RAS mutant cancers. Sci. Transl. Med. 9 (392), eaal5148.

Vasiliou, V., Pappa, A., Estey, T., 2004. Role of human aldehyde dehydrogenases in endobiotic and xenobiotic metabolism. Drug Metab. Rev. 36 (2), 279–299.

Yang, L., Shi, P., Zhao, G., Xu, J., Peng, W., Zhang, J., Zhang, G., Wang, X., Dong, Z., Chen, F., Cui, H., 2020. Targeting cancer stem cell pathways for cancer therapy. Signal Transd. Target. Ther. 5 (1), 8.

Yempalla, K.R., Munagala, G., Singh, S., Magotra, A., Kumar, S., Rajput, V.S., Bharate, S.S., Tikoo, M., Singh, G.D., Khan, I.A., Vishwakarma, R.A., Singh, P.P., 2015. Nitrofuranyl methyl piperazines as new anti-TB agents: identification, validation, medicinal chemistry, and PK studies. ACS Med. Chem. Lett. 6 (10), 1041–1046.

Zhang, N., Yin, Y., Xu, S.J., Chen, W.S., 2008. 5-Fluorouracil: mechanisms of resistance and reversal strategies. Molecules (Basel, Switzerland) 13 (8), 1551–1569.